

## Effects of structure on the liquid-glass transition

Shankar P. Das\*

*The James Franck Institute and the Department of Physics, The University of Chicago, Chicago, Illinois 60637*

(Received 1 October 1986)

We investigate the effects of liquid structure on the transport properties of dense fluids, using nonlinear fluctuating hydrodynamics. The longitudinal and shear viscosities for a Lennard-Jones system at different temperatures and pressures are computed. We find a rounded version of the transition to a glassy phase. Agreement of our results with computer simulation data is good. We also find qualitative agreement between our results and real experiments.

### I. INTRODUCTION

When a liquid is rapidly cooled below its freezing point it falls out of equilibrium and is arrested in a metastable state. The system is then said to be in a glassy phase, characterized by very long relaxation times and large viscosities. Recent studies<sup>1</sup> suggest that relaxation in glassy phases shows different types of temperature dependence ranging from Arrhenius-type behavior to much weaker power-law behavior. The latter is observed to be the case in a wide number of laboratory systems and also in computer simulations of simple systems.<sup>2,3</sup> In a recent set of papers<sup>4,5</sup> nonlinear fluctuating hydrodynamics (NFH) was used to investigate the nature of this transition. The main new result obtained was the prediction of a rounded version of the transition due to a mechanism that keeps the system ergodic at all values of the density. In these works attention was mainly focussed on the dynamic aspects of the problem. All static correlations in the system were totally ignored and the wave-number dependence in the theory was treated in a very simple way. Approaching higher densities, the structural relaxations in the supercooled state are increasingly retarded. The liquid structure, which is reflected in the wave-number dependence of the static structure factor, plays an important role here. In this paper we investigate how the dynamic mechanism, described in Refs. 4 and 5, that drives the system to a more viscous state is affected by the various contributions of the different length scales in the liquid structure. We consider a liquid that has a structure factor with a well-defined peak at the wave number  $q_0 \neq 0$ , consistent with other studies<sup>6</sup> on similar systems, and take into account the large wave-number contributions to the the viscosity. It should be pointed out here that we assume the static properties of the fluid are little affected by the transition and it is still the dynamic slowing down of the density fluctuations that is mainly responsible for the increase of the viscosity. As we will see here, we can make more detailed predictions about the "transition" than in Ref. 5.

The basic mechanism that increases the viscosity was first identified by Leutheusser<sup>7</sup> from work on kinetic theory of dense fluids. It involves a nonlinear feedback to the viscosity from the correlation of density fluctuations. A similar model was also introduced by Bengtzelius,

Götze, and Sjölander.<sup>8</sup> In Ref. 5 the same model was derived using the equations of NFH for a compressible isotropic liquid with thermal noise. The main question addressed there was: What is the dynamical behavior of a liquid if it is cooled in such a way that it always remains in a stationary state and if crystallization is avoided? The analysis focused on how the long-distance, long-time properties of the fluid will be affected by the feedback mechanism mentioned above. A careful analysis showed that for time scales that are much longer than the usual hydrodynamic regimes, the system remains ergodic for all values of the density. However, the feedback mechanism remains active over an intermediate-time scale and enhances the viscosity until nonhydrodynamic effects cut it off. As the density of the fluid increases, the hydrodynamic regime is shifted to even longer times and the system becomes more sluggish. The viscosity of the liquid increases with the increase in density but it never actually diverges. Thus, there is never a sharp transition to an ideal nonergodic glassy phase. While these works provided an insight into the basic dynamic mechanism by which the enhancement of the mode-coupling contributions to the viscosity takes place and the role of the nonlinearities in cutting off the sharp nature of the transition, no comparison of the results were made with those of real or computer experiments on similar systems. The reason for this was that all the results were stated in terms of a coupling parameter  $\lambda$  where temperature and density dependence is ill defined unless we take into account the static correlations in the system.

In this work we take the static correlation of density fluctuations in the system to be wave-vector dependent. This probes the possible effects the structure of the liquid might have on its dynamical behavior at high densities. We can then state our results in terms of physical parameters like temperature or density. We have considered here the case where the structure of the liquid is coarse grained to a length scale where only the first peak of the structure factor is relevant. This dictates our choice of the free-energy functional for the system which has an important role in determining its dynamics. The main reason for this coarse graining is that we can then work with a Gaussian free energy with gradient terms, keeping the mathematical analysis simple. As a result of having these gradient terms, we now generate a coupling between the

shear viscosity and the density fluctuations.

We will include only the hydrodynamic variables in our analysis and ignore any further complications. We believe that inclusion of energy fluctuations or some new slow variables<sup>9</sup> (e.g., the layer field displacement in a smectic-*A* liquid crystal<sup>10</sup>) in the problem might give further insight into the dynamical behavior of the liquid. We intend to investigate this in future work.

This theory requires the static structure factor for the system as a function of density and temperature as input. This is determined by the interaction potential. One could choose many different potentials and investigate how they affect the transport properties of the fluid. However, our main purpose here is to see the effects coming from different wave-number regimes. So, to keep things simple, we have considered a system interacting through a Lennard-Jones (LJ) potential. This type of system was chosen since the standard literature<sup>6</sup> contains sufficient information about the statics of such a system. Glass formation is not observed in laboratory experiments in this kind of system. However, in computer experiments, one can achieve much faster cooling rates ( $10^{11}$  K/s) and a simple LJ fluid or even a hard-sphere system can be brought into a glass phase. A number of works<sup>2</sup> have suggested a glass-transition region in the molecular dynamics and Monte Carlo simulations of such systems. These provide a good source of comparison with the predictions of our theory.

We have explicitly calculated the mode-coupling contributions to the longitudinal and shear viscosities. Our results show that the decay of the correlation of the density fluctuations, as a function of wave number, slows down considerably near the peak of the static structure factor, as was pointed out by Kirkpatrick.<sup>11</sup> We have obtained reasonable quantitative agreement between our result for the shear viscosity and that obtained from computer simulations<sup>12</sup> on similar systems at constant temperatures. Also, molecular-dynamics simulations of simple LJ liquids along the zero-pressure isobar by Clarke<sup>13</sup> show that a glass transition in such systems occurs at  $T^* = 0.29$ . [ $T$  is given in a dimensionless unit defined by Eq. (4.2).] When cooled along a zero-pressure isobar we find that at higher temperatures our data for both the shear and longitudinal viscosities fit very well to a power law form  $(T^* - T_g^*)^{-\alpha}$  with  $\alpha = 0.9$  and  $T_g^* = 0.29$ . However, at lower temperatures the sharp nature of the transition is cut off and the viscosity never actually diverges although it keeps increasing with the fall of temperature. This power-law behavior over an intermediate temperature regime also agrees qualitatively with the experimental observations by Taborék, Kleiman, and Bishop<sup>3</sup> in a number of laboratory systems.

The wave-vector dependence in the model deduced from kinetic theory was considered by other authors.<sup>14,15</sup> These works predict a sharp transition to an ideal glassy phase. In Sec. V we will refer to results obtained from such calculations.

It should be emphasized that our main goal is to get an idea about how the transition is affected by the associated structure of the liquid. For this reason we have not attempted a highly accurate description of the static struc-

ture factor. The numerical values of different quantities stated here should be considered only as reasonable approximations. Detailed descriptions of any formal development will also be avoided, since this was carried out in earlier work<sup>5</sup> on this subject.

In Secs. II and III we will describe very briefly the formal developments needed for the discussions of our results. Thus, in Sec. II we describe the equations of NFH studied and in Sec. III the field-theoretic formulation of the problem and the effect of the nonlinearities are presented. In Sec. IV we present the method we have used to calculate the static structure factor of the liquid. The main implications concerning the glass transition are described in Sec. V. In Sec. VI we summarize the main conclusions.

## II. EQUATIONS OF NONLINEAR FLUCTUATING HYDRODYNAMICS FOR COMPRESSIBLE FLUIDS

### A. Langevin equation

We start with the simplest set of hydrodynamic variables for a compressible liquid. This consists of the mass density  $\rho$ , the velocity  $\mathbf{V}$  and the momentum current density  $\mathbf{g}$ . They are constrained by the nonlinear relation

$$\mathbf{g} = \rho \mathbf{V} . \quad (2.1)$$

The dynamics of the hydrodynamic variables are governed by a generalized Langevin equation.<sup>16,17</sup> The explicit form of these equations was deduced in Ref. 5. The analysis<sup>18</sup> remains the same here and we just state the results. The equation for  $\rho$  is the continuity equation

$$\frac{\partial \rho}{\partial t} = -\nabla \cdot \mathbf{g} . \quad (2.2)$$

The equation for  $g_i$  is the generalized Navier-Stokes<sup>19</sup> equation

$$\frac{\partial g_i}{\partial t} = -\rho \nabla_i \frac{\delta F_u}{\delta \rho} - \sum_j \nabla_j (g_i g_j / \rho) - \sum_j L_{ij} (g_j / \rho) + \Theta_i . \quad (2.3)$$

Here  $F_u[\rho(\mathbf{x})]$  is the potential energy part of the effective Hamiltonian  $F$  governing the equilibrium behavior of the hydrodynamic variables. Thus we have

$$F = F_K + F_u , \quad (2.4)$$

where the kinetic energy term  $F_K$  is given<sup>20</sup> by

$$F_K = \frac{1}{2} \int d\mathbf{x} g^2(\mathbf{x}) / \rho(\mathbf{x}) . \quad (2.5)$$

The damping matrix  $L_{ij}$  is given by

$$L_{ij}(\mathbf{x}) = -\eta_0 (\frac{1}{3} \nabla_i \nabla_j + \delta_{ij} \nabla^2) - \zeta_0 \nabla_i \nabla_j , \quad (2.6)$$

where  $\eta_0$  is the bare shear viscosity and  $\zeta_0$  the bare bulk viscosity. We define the bare longitudinal viscosity  $\Gamma_0 = \zeta_0 + 4\eta_0/3$ . The noise  $\Theta_j$  is Gaussian and satisfies

$$\langle \Theta_i(\mathbf{x}, t) \Theta_j(\mathbf{x}', t') \rangle = 2k_B T L_{ij}(\mathbf{x}) \delta(\mathbf{x} - \mathbf{x}') \delta(t - t') . \quad (2.7)$$

The first term on the right-hand side (RHS) of Eq. (2.3) gives the force term in the Navier-Stokes equation while the second term is the usual convective term as it appears normally in the equation for  $g_i$ . The set of equations (2.2) and (2.3) together with the nonlinear constraint (2.1) governs the dynamics of the hydrodynamic variables in our model. However, the first term on the RHS of Eq. (2.3) will be determined by the form of  $F_u$  in the free-energy functional. We consider this next.

### B. Free energy

The static properties of the system are determined by its free-energy functional. Thus, in general, the equilibrium averages of the fields  $\Psi_i$  at equal times are given by

$$\langle \Psi_i \Psi_j \rangle \equiv \int D(\Psi) e^{-\beta F[\Psi]} \Psi_i \Psi_j / Z, \quad (2.8)$$

where

$$Z = \int D(\Psi) e^{-\beta F[\Psi]} \quad (2.9)$$

is the partition function,  $\beta = (k_B T)^{-1}$  and  $D(\Psi)$  indicates a functional integral over the fields  $\Psi_i$ . For our purpose here, we will select a free-energy functional that gives rise to a static structure factor similar to that observed in real liquids. As was noted in the Introduction, we take into consideration only the first peak in the observed structure factor. This amounts to a coarse graining of the system. A large wave-number cutoff  $\Lambda$  thus naturally enters into

the theory. In this paper we will work with the free energy,

$$F = \frac{1}{2} \int d\mathbf{x} \left[ A [\delta\rho(\mathbf{x})]^2 + \kappa [\delta\rho(\mathbf{x}) (\nabla^2 + q_0^2) \delta\rho(\mathbf{x})] + \frac{\mathbf{g}^2(\mathbf{x})}{\rho(\mathbf{x})} \right], \quad (2.10)$$

where  $\delta\rho(\mathbf{x}) = \rho(\mathbf{x}) - \rho_0$ .  $A$  and  $\kappa$  are functions of density and temperature. Clearly there is nothing unique about this choice of the free-energy functional but it is technically advantageous since it is quadratic in the density fluctuations. To avoid technical complications we will assume that the  $1/\rho$  factor in the kinetic energy term does not influence the statics.

Using Eq. (2.10) in Eq. (2.8), we obtain a static structure factor

$$\chi_{\rho\rho}(q) = \frac{1}{A + \kappa(q^2 - q_0^2)^2}, \quad (2.11)$$

where  $\chi_{\rho\rho}(q)$  is the Fourier transform of  $\langle \delta\rho(\mathbf{x}) \delta\rho(\mathbf{x}') \rangle$ . Now using Eqs. (2.5), (2.6), and (2.10), we can write Eq. (2.3) in terms of a stress tensor  $\sigma_{ij}$ ,

$$\frac{\partial g_i}{\partial t} = - \sum_j \nabla_j \sigma_{ij} + \Theta_i. \quad (2.12)$$

The stress tensor  $\sigma_{ij}$  can be divided into a reversible part  $\sigma_{ij}^R$  and a dissipative part  $\sigma_{ij}^D$  which are given by

$$\begin{aligned} \sigma_{ij}^R = & \frac{g_i g_j}{\rho} + \frac{\delta_{ij}}{2} (\chi_{\rho\rho}^{-1}(0) (\delta\rho)^2 + \kappa \{ [\nabla^2 (\delta\rho)]^2 - 2 [\nabla (\delta\rho)] \cdot [\nabla (\nabla^2 + q_0^2) (\delta\rho)] \}) \\ & + \kappa [\delta\rho \nabla_i \nabla_j (\nabla^2 + q_0^2) (\delta\rho) + \nabla_i \nabla_j (\delta\rho) (\nabla^2 + q_0^2) \delta\rho] \end{aligned} \quad (2.13)$$

and

$$\sigma_{ij}^D = \eta_0 [\nabla_i V_j + \nabla_j V_i - \frac{2}{3} \delta_{ij} (\nabla \cdot \mathbf{V})] - \zeta_0 \delta_{ij} (\nabla \cdot \mathbf{V}). \quad (2.14)$$

It is useful to note here that the symmetry  $\sigma_{ij} = \sigma_{ij}^R + \sigma_{ij}^D = \sigma_{ji}$  ensures conservation of angular momentum.

## III. FIELD-THEORETICAL FORMULATION

### A. The Martin-Siggia-Rose formalism

In order to investigate what effects the nonlinearities in the equations developed in Sec. II have on the transport properties of the system, we need to develop a formalism convenient for renormalizing the linear theory. We will use for this purpose the Martin-Siggia-Rose<sup>21</sup> (MSR) formalism which is standard in the literature for studying the statistical properties of a classical system. The formal development needed is identical with the work done in Ref. 5. We have to introduce a set of conjugate fields  $\hat{\rho}$ ,  $\hat{g}_i$ , and  $\hat{V}_i$  corresponding to the original fields  $\rho$ ,  $g_i$ , and  $V_i$ , respectively. Here we will only state the new form of the MSR action expressed as a symmetric function of the hatted and the unhatted variables. Let  $\Psi_\alpha(1)$  be a vector where  $\alpha$  runs over  $\rho$ ,  $\hat{\rho}$ ,  $g_i$ ,  $\hat{g}_i$ ,  $V_i$ , and  $\hat{V}_i$  and 1 labels space  $x_1$  and time  $t_1$ . The action can then be written in the following form:

$$\begin{aligned} A[\Psi] = & \frac{1}{2} \int d1 \int d2 \sum_{\alpha, \beta} \Psi_\alpha(1) [G_0^{-1}(1,2)]_{\alpha\beta} \Psi_\beta(2) + \frac{1}{3} \int d1 \int d2 \int d3 \sum_{\alpha, \beta, \gamma} V_{\alpha\beta\gamma}(1,2,3) \Psi_\alpha(1) \Psi_\beta(2) \Psi_\gamma(3) \\ & + \frac{1}{4} \int d1 \int d2 \int d3 \int d4 \sum_{\alpha, \beta, \gamma, \mu} V_{\alpha, \beta, \gamma, \mu}(1,2,3,4) \Psi_\alpha(1) \Psi_\beta(2) \Psi_\gamma(3) \Psi_\mu(4), \end{aligned} \quad (3.1)$$

where the  $G_0^{-1}(1,2)$  corresponds to the Greens functions in the linearized theory. We give the space-time Fourier trans-

form  $[G_0^{-1}(q, \omega)]_{\alpha\beta}$  of this matrix in Table I. The wave-vector-dependent speed of sound,  $c_0(q)$ , shown there has an explicit form

$$c_0^2(q) = \rho_0 [A + \kappa(q^2 - q_0^2)^2] = \rho_0 \chi_{\rho\rho}^{-1}(q). \quad (3.2)$$

The symmetrized cubic vertices are given by

$$V_{\alpha\beta\gamma}(1, 2, 3) = \frac{1}{2} [\tilde{V}_{\alpha\beta\gamma}(1, 2, 3) + \tilde{V}_{\beta\alpha\gamma}(2, 1, 3) + \tilde{V}_{\gamma\beta\alpha}(3, 2, 1) + \tilde{V}_{\alpha\gamma\beta}(1, 3, 2) + \tilde{V}_{\beta\gamma\alpha}(2, 3, 1) + \tilde{V}_{\gamma\alpha\beta}(3, 1, 2)], \quad (3.3)$$

where

$$\tilde{V}_{\alpha\beta\gamma}(1, 2, 3) = \sum_{i=1}^3 \tilde{V}_{\alpha\beta\gamma}^{(i)}(1, 2, 3). \quad (3.4)$$

The unsymmetrized vertices  $\tilde{V}_{\alpha\beta\gamma}^{(i)}(1, 2, 3)$  are given by

$$\begin{aligned} \tilde{V}_{\alpha\beta\gamma}^{(1)}(1, 2, 3) = & i \sum_i \delta_{\alpha, \hat{g}_i} \nabla_j^{(1)} \{ \delta_{ij} [\frac{1}{2} \chi_{\rho\rho}^{-1}(q) \delta(1, 2) \delta(1, 3) - \kappa \nabla^2 \delta(1, 2) \nabla^2 \delta(1, 3)] \\ & + \kappa [\delta_{ij} \delta(1, 2) \nabla^2 - \nabla_i \delta(1, 2) \nabla_j + \nabla_i \nabla_j \delta(1, 2)] (\nabla^2 + q_0^2) \delta(1, 3) \} \delta_{\beta, \rho} \delta_{\gamma, \rho} \end{aligned} \quad (3.5)$$

from the term nonlinear in  $\delta\rho$ ,

$$\tilde{V}_{\alpha\beta\gamma}^{(2)}(1, 2, 3) = i \rho_0 \sum_{i,j} \delta_{\alpha, \hat{g}_i} \nabla_j^{(1)} \delta_{\beta, v_i} \delta_{\gamma, v_j} \delta(1, 2) \delta(1, 3) \quad (3.6)$$

from the convective term, and

$$\tilde{V}_{\alpha\beta\gamma}^{(3)}(1, 2, 3) = -i \sum_i \delta_{\alpha, \hat{v}_i} \delta_{\beta, \rho} \delta_{\gamma, v_i} \quad (3.7)$$

from the nonlinear constraint  $\mathbf{g} = \rho \mathbf{V}$ . The symmetrized quartic vertex is one-sixth the sum of all pairwise permutations of the set of variables  $(\alpha, 1)$ ,  $(\beta, 2)$ ,  $(\gamma, 3)$ , and  $(\mu, 4)$  labeling the unsymmetrized vertex  $\tilde{V}_{\alpha\beta\gamma\mu}(1, 2, 3, 4)$  where

$$\begin{aligned} \tilde{V}_{\alpha\beta\gamma\mu}(1, 2, 3, 4) = & - \sum_{i,j} \delta_{\alpha, \hat{g}_i} \delta_{\beta, \rho} \delta_{\gamma, v_i} \delta_{\mu, v_j} \\ & \times \nabla_{i,j}^{(1)} (\delta(1, 2) \delta(1, 3) \delta(1, 4)). \end{aligned} \quad (3.8)$$

### B. Effect of the nonlinearities

The Green function in the full nonlinear theory is given by the following Dyson-type equation:

$$G^{-1}(1, 2) = G_0^{-1}(1, 2) - \Sigma(1, 2). \quad (3.9)$$

Thus the correction due to the nonlinearities is obtained through the self-energy  $\Sigma$ . As there are a large number of fields, the matrix of the Greens functions gets quite involved. However, we can treat the transverse and the lon-

gitudinal components of the fields  $\mathbf{g}, \mathbf{V}$  and their hatted counterparts separately making the analysis slightly simpler. We can split the  $G$ 's into their longitudinal and transverse parts

$$G_{\alpha, \beta_j}(\mathbf{q}, \omega) = \hat{q}_i \hat{q}_j G_{\alpha\beta}^L(\mathbf{q}, \omega) + (\delta_{ij} - \hat{q}_i \hat{q}_j) G_{\alpha\beta}^T(\mathbf{q}, \omega). \quad (3.10)$$

Similarly the  $\Sigma$ 's can also be split into  $\Sigma^L$  and  $\Sigma^T$ . These self-energies were analyzed in considerable detail in Ref. 5 and several relations among them were established. In the small  $q$  and  $\omega$  limit, the correlation functions  $G_{\psi\psi}$  were expressed in terms of the corresponding response functions  $G_{\psi\hat{\psi}}$ . In the following we will state some of those results in a more generalized form that will be useful for our later analysis.

(i) The transverse velocity correlation function  $G_{vv}^T$  can be computed as

$$G_{vv}^T(q, \omega) = -2\beta^{-1} \text{Im} G_{v\hat{g}}^T, \quad (3.11)$$

where the response function  $G_{v\hat{g}}^T$  is given by

$$G_{v\hat{g}}^T(q, \omega) = \frac{1}{\rho_T \omega + i q^2 \eta(q, \omega)} \quad (3.12)$$

with

$$\rho_T = \rho_0 - i \Sigma_{\hat{v}\hat{v}}^T(q, \omega), \quad (3.13)$$

$$q^2 \eta(q, \omega) = q^2 \eta_0 + i \Sigma_{\hat{g}\hat{v}}^T(q, \omega). \quad (3.14)$$

Equation (3.14) gives the renormalization for the bare shear viscosity  $\eta_0$ .

(ii) The correlation function  $G_{\rho\rho}$  can be computed as

$$G_{\rho\rho}(q, \omega) = -2\beta^{-1} \chi_{\rho\rho}(q) \text{Im} G_{\rho\hat{\rho}}(q, \omega), \quad (3.15)$$

where the response function  $G_{\rho\hat{\rho}}(q, \omega)$  is given by

$$G_{\rho\hat{\rho}}(q, \omega) = \frac{\rho_L \omega + i \Gamma(q, \omega)}{\rho_L (\omega^2 - q^2 c^2) + i \Gamma(q, \omega) [\omega + i q \Sigma_{\hat{v}\hat{\rho}}^L(q, \omega)]} \quad (3.16)$$

TABLE I. Entries of the inverse  $(G_0^{-1})_{\alpha\beta}$  of the zeroth-order matrix  $G_0$ .

	$\rho$	$g_j$	$v_j$	$\hat{\rho}$	$\hat{g}_j$	$\hat{v}_j$
$\rho$	0	0	0	$-\omega$	$q_j c_0^2(q)$	0
$g_i$	0	0	0	$q_i$	$-\omega \delta_{ij}$	$i \delta_{ij}$
$v_i$	0	0	0	0	$i L_{ij}$	$-i \rho_0 \delta_{ij}$
$\hat{\rho}$	$\omega$	$-q_j$	0	0	0	0
$\hat{g}_i$	$-q_i c_0^2(q)$	$\omega \delta_{ij}$	$i L_{ij}$	0	$2\beta^{-1} L_{ij}$	0
$\hat{v}_i$	0	$i \delta_{ij}$	$-i \rho_0 \delta_{ij}$	0	0	0

and

$$\Gamma(q, \omega) = q^2 \Gamma_0 + i \Sigma_{\hat{g}v}^L(q, \omega), \quad (3.17)$$

$$qc^2(q, \omega) = qc_0^2 + \Sigma_{\hat{g}\rho}^L(q, \omega), \quad (3.18)$$

$$\rho_L(q, \omega) = \rho_0 - i \Sigma_{\hat{v}v}^L(q, \omega). \quad (3.19)$$

Equations (3.17) and (3.18) give the renormalized longitudinal viscosity and the sound speed, respectively. We believe the  $q$  and  $\omega$  dependence of  $\rho_L$  and  $\rho_T$  are not very important here. We will replace these quantities by their zeroth-order values,  $\rho_L(0,0)$  and  $\rho_T(0,0)$  and for practical purposes take both of them equal to the physical density.

(iii) Next we consider the quantity  $\Sigma_{\hat{v}_i \hat{v}_j}(\mathbf{q}, \omega)$ . Note that this self-energy arises from the nonlinear constraint (2.1). Its role in cutting off the sharp nature of the transition was discussed in Ref. 5. A relation between  $\Sigma_{\hat{v}_i \hat{v}_j}$  and  $\Sigma_{\hat{v}_i \hat{v}_j}$  was established there and it is given by Eq. (6.65). This result was proved for small  $q$  and  $\omega$  to all orders of perturbation theory. Here we will assume that the corresponding result for finite  $q$  and  $\omega$  also holds true. This can be written as

$$q_i \Sigma_{\hat{v}_i \hat{v}_j}(\mathbf{q}, \omega) = \frac{c_i q_j}{2\beta^{-1}\rho} c^2(q) \Sigma_{\hat{v}_i \hat{v}_j}(\mathbf{q}, \omega) \equiv q^2 [\tilde{\gamma}(\mathbf{q}, \omega)]. \quad (3.20)$$

We believe that at this level of sophistication this is a reasonable assumption in estimating the large-wave-number effects in the theory. The task of testing corrections to these assumptions for finite  $q$  and  $\omega$  remains a matter of further research.

### C. One-loop contributions

We have listed above in Eqs. (3.14) and (3.17) the renormalization of the shear and the longitudinal viscosities.

---


$$\Gamma^{(m)}(q, t) = \int dk k^2 \int_{-1}^{+1} du \{ \chi^{-1}(\mathbf{q}-\mathbf{k}) + \kappa(2ku - q)[q(\mathbf{q}-\mathbf{k})^2 - 2ku(q_0^2 - k^2)] \}^2 G_{\rho\rho}(k, t) G_{\rho\rho}(|\mathbf{q}-\mathbf{k}|, t) \quad (3.25)$$

and

$$\begin{aligned} \eta^{(m)}(q, t) &= \int dk k^2 \int_{-1}^{+1} du [\kappa(2ku - q)(q_0^2 - k^2)k]^2 (1-u^2) \\ &\quad \times G_{\rho\rho}(k, t) G_{\rho\rho}(|\mathbf{q}-\mathbf{k}|, t), \end{aligned} \quad (3.26)$$

where  $u_1 = \hat{\mathbf{q}} \cdot (\mathbf{q}-\mathbf{k}) / |\mathbf{q}-\mathbf{k}|$  and  $u = \hat{\mathbf{q}} \cdot \hat{\mathbf{k}}$ . Note that in writing down (3.25) and (3.26) we have transformed the time into a dimensionless form by letting

$$t \rightarrow t \frac{\Gamma_0}{\rho c^2}. \quad (3.27)$$

Also, we have absorbed the contributions to the corresponding self-energies coming from the convective vertex

We use the diagrammatic expansion discussed in Ref. 5 to obtain the contributions to the self-energies to one-loop order, the nonlinear vertices involved in the calculation are listed in Eqs. (3.5)–(3.8). We are using a static structure factor given by

$$\chi_{\rho\rho}(q) = \begin{cases} \frac{1}{A + \kappa(q^2 - q_0^2)^2} & \text{for } q \leq \Lambda \\ 0 & \text{for } q > \Lambda, \end{cases} \quad (3.21a)$$

$$(3.21b)$$

where  $\Lambda$  serves as a large wave-number cutoff.

The renormalized shear and longitudinal viscosities can be written in the form

$$\Gamma(q, \omega) = \Gamma_0 \left[ 1 + \lambda \int_0^\infty dt e^{i\omega t} \Gamma^{(m)}(q, t) \right] \quad (3.22)$$

and

$$\eta(q, \omega) = \Gamma_0 \left[ \frac{\eta_0}{\Gamma_0} + \lambda \int_0^\infty dt e^{i\omega t} \eta^{(m)}(q, t) \right]. \quad (3.23)$$

$\lambda$  is a dimensionless parameter related to the temperature and density of the liquid in the following way:

$$\lambda = \frac{k_B T \Lambda^3}{\rho c^2}, \quad (3.24)$$

where  $c = c(q=0)$ .  $\Gamma^{(m)}(q, t)$  and  $\eta^{(m)}(q, t)$  are the contributions to the respective transport coefficients due to the coupling of the density fluctuation modes. We obtain the following expressions for  $\Gamma^{(m)}(q, t)$  and  $\eta^{(m)}(q, t)$  at the one-loop order:

---

(3.6) as renormalizations of the bare viscosities  $\eta_0$  and  $\Gamma_0$ , respectively. This is done since we want to focus our attention on the contributions coming only from the coupling of density fluctuation modes. It is known from the study<sup>22</sup> of incompressible fluids that in three dimensions the convective vertex has finite contributions to the transport coefficients while for two or less dimensions it gives rise to divergences and conventional hydrodynamics breaks down. Thus in low-dimensional systems such contributions must be treated carefully and will compete with the feedback mechanism coming from the nonlinearities which are solely due to density fluctuations. So our analysis here applies to three-dimensional systems only.

Finally, we obtain the following expression for  $\Sigma_{\rho\hat{v}}(\mathbf{q}, \omega)$  from Eq. (3.20) by computing  $\Sigma_{\hat{v}_i \hat{v}_j}(\mathbf{q}, \omega)$  to one-loop order,

$$q \Sigma'_{\rho\delta}(\mathbf{q}, \omega) = \frac{q^2 c^2(q)}{2\beta^{-1}\rho} \{ (1-u^2)[G_{vv}^T(k, \Omega) + G_{vv}^L(k, \Omega)]G_{\rho\rho}(|\mathbf{q}-\mathbf{k}|, \omega-\Omega) + uu_1 G_{\rho v}^L(|\mathbf{q}-\mathbf{k}|, \omega-\Omega)G_{v\rho}^L(k, \Omega) \} . \quad (3.28)$$

This completes the formal development we needed for the realization of our model. At this stage we have reached a coupled set of equations (3.11), (3.16), and (3.20) consisting of  $G_{\rho\rho}$  and  $G_{vv}^T$ . We will solve these equations numerically in the time domain to obtain the behavior of the density-correlation function. The latter can then be used to compute the mode-coupling contributions to the transport coefficients given by Eqs. (3.22) and (3.23). Before discussing this, we need to know the values of the phenomenological parameters  $A, \kappa, q_0$  for the fluid as functions of temperature and density. This is considered next.

#### IV. STATIC STRUCTURE FACTOR

To make any quantitative statement in our theory we need to know the values of the parameters  $A, \kappa$ , and  $q_0$  in the free energy introduced in Eq. (2.10). In other words, we need the  $\chi_{\rho\rho}(q)$  for the liquid as a function of density and temperature. For this purpose we will consider a simple monoatomic liquid interacting through a Lennard-Jones (LJ) potential which is given by

$$w(r) = 4\epsilon \left[ \left( \frac{\sigma}{r} \right)^{12} - \left( \frac{\sigma}{r} \right)^6 \right] . \quad (4.1)$$

Here  $\sigma$  has the dimensions of length and  $\epsilon$  has dimensions of energy. Henceforth, we will use the following dimensionless representations for the number density  $n$ , the pressure  $P$ , and the temperature  $T$  of the liquid:

$$\rho^* = n\sigma^3, \quad P^* = \frac{P\sigma^3}{\epsilon}, \quad \text{and} \quad T^* = \frac{1}{\beta\epsilon} . \quad (4.2)$$

Here we will briefly sketch the procedure we have used for calculating the static structure factor. This was first described by Weak, Chandler, and Anderson.<sup>23</sup> In this approach the LJ potential is split into a harshly repulsive part  $u_0(r)$  and an attractive part  $u(r)$  defined by

$$u_0 = \begin{cases} w(r) + \epsilon, & r \leq 2^{1/6}\sigma \\ 0, & r > 2^{1/6}\sigma \end{cases} \quad (4.3a)$$

$$(4.3b)$$

and

$$u(r) = \begin{cases} -\epsilon, & r \leq 2^{1/6}\sigma \\ w(r), & r > 2^{1/6}\sigma . \end{cases} \quad (4.4a)$$

$$(4.4b)$$

Now we replace the system by a trial system in which the pair potential is given by

$$w_T(r) = u_d(r) + u_T(r) , \quad (4.5)$$

where

$$u_T(r) = u(r) \quad \text{for } r \geq d , \quad (4.6a)$$

$$u_d(r) = \begin{cases} \infty & \text{for } r < d \\ 0 & \text{for } r \geq d , \end{cases} \quad (4.6b)$$

$$(4.6c)$$

and  $d \leq 2^{1/6}\sigma$ . It is quite straightforward to show that the structure factor in the actual system is approximately given by

$$\chi_{\rho\rho}(q) = \chi_{\rho\rho}^T(q) + \rho \int d\mathbf{r} g_T(r) e^{\beta w_T(r)} \times (e^{-\beta w(r)} - e^{-\beta w_T(r)}) \exp(-i\mathbf{q}\cdot\mathbf{r}) , \quad (4.7)$$

where  $\chi_{\rho\rho}^T(q)$  is the structure factor in the trial system and  $g_T(r)$  is the pair-distribution function<sup>24</sup> for it. Equation (4.7) implies that we can calculate the structure factor for the original system in terms of the properties of the trial system. Note that in the trial system the repulsive potential was replaced by a hard-sphere potential. The main reason for going over to this trial system lies in the fact that a great deal of information is available for hard-sphere systems. Thus as the simplest approximation we neglect the attractive potential  $u_T$  entirely and consider a hard-sphere system as the trial system. However, the hard-sphere diameter  $d$  is an open parameter here. Its value is chosen such that the compressibility  $\chi_{\rho\rho}(q=0)$  for the original and the trial systems are equal. Under that condition the Helmholtz free energy for the two systems agrees to fourth order in a perturbation theory.<sup>23</sup> It should be noted that we are interested in the structure of the liquid at high density and hence the major contribution to it comes from the repulsive part of the pair potential. Thus we will take the structure factor for our system to be that of a hard-sphere whose diameter is equal to the value of  $d$  given above. For the hard-sphere system we have used the Wertheim-Thiele<sup>25</sup> solution of the Percus-Yevick equation<sup>24</sup> with the corrections proposed by Verlet and Weiss.<sup>26,27</sup> Indeed, for a highly accurate value of  $\chi_{\rho\rho}(q)$ , especially at high temperature and low density, one needs to take into account the perturbative corrections coming from the attractive part of the pair potential and follow the procedures outlined in Ref. 23. However, as was noted in the Introduction, we have not worked here for such accuracy. The compressibility factor  $\beta P/\rho$  and hence the pressure  $P$  is evaluated up to first order in the perturbation theory. We have used the Carnahan-Starling<sup>28</sup> equation for the compressibility factor of the reference hard-sphere system.

Now we choose the values of  $A, \kappa$ , and  $q_0$  such that the functional form (2.11) for the structure factor of the liquid

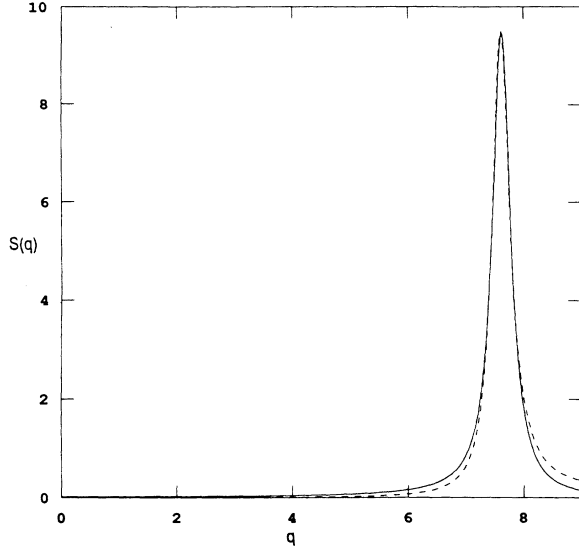


FIG. 1. Structure factor at  $T^*=0.20$  and  $P^*=0$  and the corresponding curve given by Eq. (2.11). The solid line indicates the results obtained with the method outlined in Sec. IV while the dashed line shows the best-fit curve.

is a best fit to the values of  $\chi_{\rho\rho}(q)$  calculated in the above analysis. In Table II we give a set of values for those parameters as a function of temperature and density. It is interesting to note that while the width and the height of the first peak changes sharply with density, the position of the peak changes very slightly. This indicates that the dominant length scale in the liquid structure is chosen at densities much lower than that corresponding to super-cooled regions or to crystallization. In Fig. 1 we show the structure factor of the liquid at  $\rho^*=1.05$  and  $T=0.20$  and the best fit to this curve with a proper choice of  $A$ ,  $q_0$ , and  $\kappa$ . We take the value for the upper cutoff in the wave-vector integrations close to the first minimum in the structure-factor peak since the approximation for  $S(q)$  given by Eq. (2.11) is best up to that region.

TABLE II. The best-fit values of parameters  $A$ ,  $\kappa$ , and  $q_0$  for the structure-factor curve along the  $P^*=0$  isobar.

$T^*$	$\rho^*$	$A$	$\kappa$	$q_0$
0.20	1.055	0.1054	0127	7.62
0.24	1.037	0.1233	0111	7.55
0.28	1.020	0.1415	0099	7.49
0.32	1.003	0.1604	0088	7.43
0.36	0.990	0.1800	0079	7.38
0.40	0.970	0.1995	0072	7.33
0.44	0.953	0.2208	0065	7.28
0.48	0.937	0.2404	0060	7.23
0.52	0.920	0.2611	0055	7.19
0.56	0.904	0.2811	0050	7.15

## V. IMPLICATIONS FOR THE GLASS TRANSITION

Our main goal in this section is to compute the mode-coupling contributions to the longitudinal and shear viscosities coming from the density-fluctuation modes. Expressions for these contributions up to one-loop order are given by Eqs. (3.22) and (3.23), respectively. In Sec. IV we described in detail how we determine the static parameters  $A$ ,  $\kappa$ , and  $q_0$  necessary for this calculation. The next step is to find out the time-dependent behavior of the correlation function  $G_{\rho\rho}(q, t)$ . For this purpose we define two functions  $\Psi$  and  $\phi$  related to the density and momentum correlations in the following way:

$$\Psi(q, t) = \frac{G_{\rho\rho}(q, t)}{\chi_{\rho\rho}(q)}, \quad (5.1)$$

$$\phi(q, t) = \frac{G_{vv}^T(q, t)}{\chi_{vv}^T(q)}, \quad (5.2)$$

where  $\chi_w^T$  is the equal-time transverse velocity correlation and is equal to  $\beta^{-1}/\rho$ . Now we take the inverse Laplace transform of Eqs. (3.12) and (3.16) to obtain the following two integral differential equations for  $\Psi$  and  $\phi$ , respectively:

$$\begin{aligned} \dot{\Psi}(q, t) + q^2 \lambda_1 \left\{ \dot{\Psi}(q, t) + \lambda \left[ \int_0^t d\tau \dot{\Psi}(q, t-\tau) \Gamma^{(m)}(q, \tau) \right. \right. \\ \left. \left. + q^2 \int_0^t d\tau \gamma(q, t-\tau) \left[ \Psi(q, \tau) + \lambda \int_0^\tau d\tau' \Gamma^{(m)}(q, \tau-\tau') \psi(q, \tau') \right] \right] \right\} = 0, \quad (5.3) \end{aligned}$$

$$\dot{\phi}(q, t) + \lambda_1 q^2 \left[ \frac{\eta_0}{\Gamma_0} \phi(q, t) + \lambda \int_0^t \eta^{(m)}(q, t-\tau) \phi(q, \tau) d\tau \right] = 0, \quad (5.4)$$

where

$$\lambda_1 = \frac{\Gamma_0^2 \Lambda^2}{\rho^2 c^2} \quad (5.5)$$

and  $\lambda$  is the dimensionless parameter defined in Eq. (3.24). Note that  $\lambda$  in this case is quite different from the one described in Ref. 5. In this case it decreases as we decrease the temperature. The dot in Eqs. (5.3) and (5.4) refers to derivative with respect to time. In Eq. (5.3) the quantity  $\gamma(q, t)$  is obtained from the inverse Laplace transform of  $\tilde{\gamma}(q, \omega)$  defined in Eq. (3.20). Using Eq. (3.28) we get the following expression for  $\gamma(q, t)$  to one-loop order:

$$\gamma(q,t) = \frac{1}{2} \int dk k^2 \int_{-1}^{+1} du \frac{\chi_{\rho\rho}(|\mathbf{q}-\mathbf{k}|)}{\chi_{\rho\rho}(0)} \left[ \lambda_1(1-u^2)\Psi(|\mathbf{q}-\mathbf{k}|,t)\phi(k,t) + \frac{\chi_{\rho\rho}(k)}{\chi_{\rho\rho}(0)} \frac{\Psi(|\mathbf{q}-\mathbf{k}|,t)}{|\mathbf{q}-\mathbf{k}|} \frac{\Psi(k,t)}{k} \left[ u_1 + u \frac{|\mathbf{q}-\mathbf{k}|}{k} \right] \right], \quad (5.6)$$

where  $u$  and  $u_1$  were defined with Eq. (3.26).

Thus, we have reached a complete set of coupled differential equations given by (5.3), (5.4), and (5.6) which determines the decay of the correlation functions  $\Psi(q,t)$  and  $\phi(q,t)$  with time. We solve these equations numerically subject to the initial conditions  $\phi(q,t=0) = \Psi(q,t=0) = 1$  and  $\dot{\Psi}(q,t=0) = 0$  for all values  $q$  up to  $\Lambda$ . For the bare viscosities  $\Gamma_0$  and  $\eta_0$  we assume the Enskog forms<sup>29</sup> for a hard-sphere system with diameter equal to the optimum value  $d$  described in Sec. IV.

We now substitute  $\Psi(q,t)$  back into expressions (3.22) and (3.23) to obtain the mode-coupling contributions to the longitudinal and the shear viscosity. Figure 2 shows the time decay of  $\Psi$  for different values of the wave vector  $q$  at  $\rho^* = 1.055$  and  $P^* = 0$ .

The slowing down of the decay of density fluctuations near the static-structure-factor peak is well known in the literature<sup>30</sup> and this is further enhanced here by the mode-coupling effects. The dynamic slowing down at finite values of  $q$  indicates how the microscopic structure of the liquid contributes to the mode-coupling integrals involved in the transport coefficients.

In describing our results we will refer to a dimensionless form for the longitudinal and the shear viscosity given, respectively, by

$$\Gamma^* = \Gamma[\sigma^2(mk_B T)^{-1/2}] \quad \text{and} \quad \eta^* = \eta[\sigma^2(mk_B T)^{-1/2}].$$

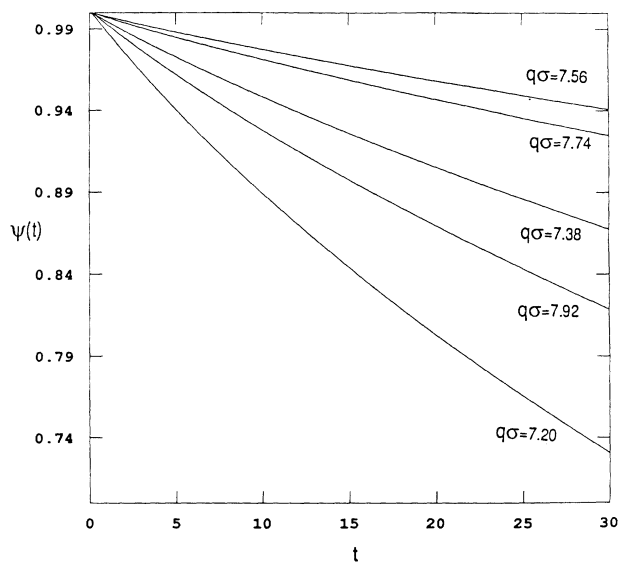


FIG. 2. Behavior of the density correlation function  $\Psi(q,t)$  in time for different values of  $q$  near the first peak in the structure factor at  $\rho^* = 1.055$  and  $P^* = 0$ .

In Fig. 3 we plot our result for  $\Gamma(q, \omega=0)$  at  $T^* = 0.48$  and  $P^* = 0$ , as a function of  $q\sigma$ . For large wave numbers the transport coefficient is small which is physically sensible. For very small lengths the transport coefficients go to their values calculated from short-time properties of the liquid. The molecules get trapped in cages and transport over such small-length scales is expected to be less effected by supercooling. At some intermediate-length scale, still microscopic, there appears to be some kind of freezing taking place which persists to the hydrodynamic length scales corresponding to  $q=0$ . The peak in Fig. 3 reflects the structural effects in the transport properties of the liquid. Since experimental measurements correspond to transport properties of the fluid at macroscopic length scales, for the rest of this section we will focus our attention on the results at  $q=0$ . We have calculated the quantities  $\Gamma(q=0, \omega=0)$  and  $\eta(q=0, \omega=0)$  at several values of density and temperature. Our main results are as follows.

(i) Calculation at a constant temperature. First we calculate the shear viscosity as a function of the density keeping the temperature constant at  $T = 1.5$ . This is plotted in Fig. 4. We compare this result with the shear viscosities obtained from molecular-dynamics simulations<sup>12</sup> of similar systems. For intermediate values of density the agreement is good. At very low densities, however, the agreement looks poor, possibly because the

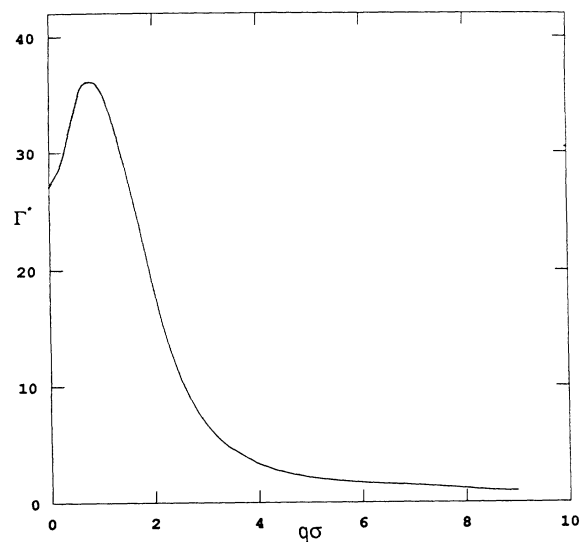


FIG. 3. Mode-coupling contribution to the longitudinal viscosity as a function of the wave number at  $T^* = 0.48$  and  $P^* = 0$ .

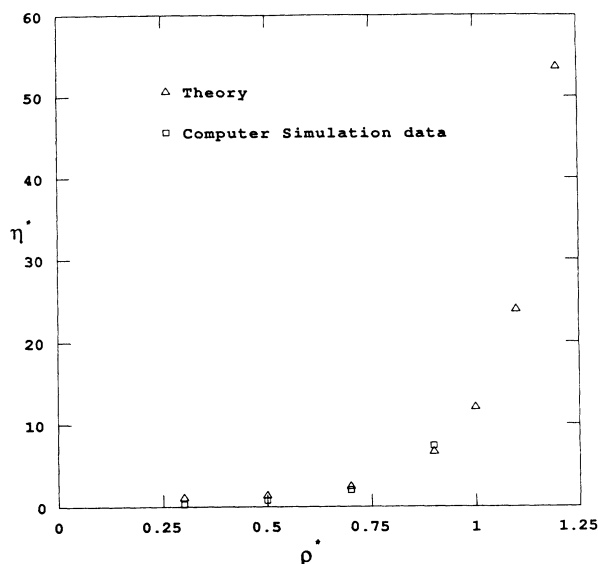


FIG. 4. Shear viscosity of the liquid compressed at a constant temperature  $T^* = 1.5$  as a function of the density. The results obtained from computer simulations up to intermediate values of the density are also shown.

starting point in our analysis was the approximation (2.11) for the structure factor of the liquid, which is not good at such low densities. As the density is increased (for  $\rho^* > 1.0$ ) we do see a substantial enhancement in the shear viscosity due to mode-coupling contributions.

(ii) Calculation at constant pressure. Most laboratory glasses are produced by cooling at a constant pressure, so we consider a Lennard-Jones system cooled at a constant pressure  $P^* = 0$ . The calculated values of the shear and longitudinal viscosities as a function of temperature are listed in Table III. We find that for  $T^* > 0.35$  the data for both the shear and longitudinal viscosities agree very well with the power-law form  $(T^* - 0.29)^{-\alpha}$  with  $\alpha = 0.9$ . As one approaches lower temperatures (hence higher densities) the sharp nature of the transition is cut off, i.e., the viscosity keeps increasing but always remains finite. In Fig. 5 we show the behavior of the quantity  $\tilde{\gamma}(0,0)$  in Eq. (3.20) with temperature. As the temperature is lowered this quantity becomes smaller, showing that the diffusive

TABLE III. The longitudinal and shear viscosities calculated along the zero-pressure isobar.

$T^*$	$\rho^*$	$\Gamma^*$	$\eta^*$
0.20	1.0550	241.7138	82.6857
0.24	1.0370	185.5153	68.6333
0.28	1.0200	159.0556	52.6447
0.32	1.0030	117.8771	41.1245
0.36	0.9859	81.5944	30.1606
0.40	0.9697	57.6154	20.7921
0.44	0.9520	41.9876	15.5925
0.48	0.9366	33.8791	12.8525
0.52	0.9203	27.9785	10.8410
0.56	0.9041	23.4660	9.2758

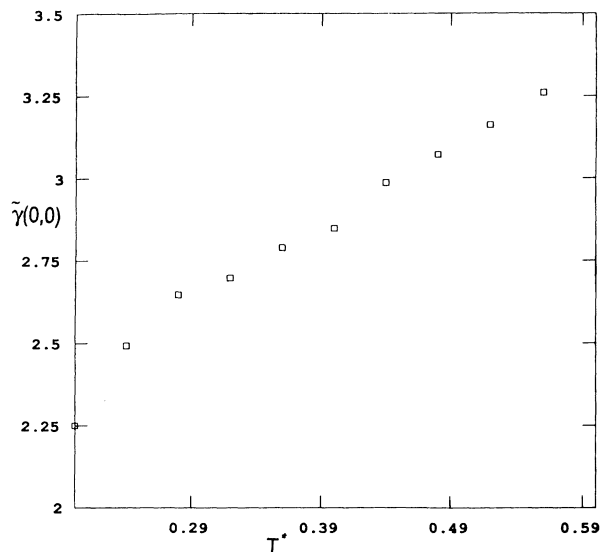


FIG. 5.  $\tilde{\gamma}(0,0)$  vs temperature along the zero-pressure isobar.

mode discovered in Ref. 5 is getting slower. In order to demonstrate the cutoff nature of the transition we plot the inverse of the viscosities and also their power-law fits for the high-temperature regions are shown in Figs. 6 and 7. The nature of these curves is qualitatively rather similar to the behavior of several laboratory systems described in Ref. 3. There it was claimed that for an intermediate-temperature regime higher than the usual glass-transition region, the viscosity has a power-law behavior with a nonuniversal exponent, and that the value of this exponent ranges from 1.5 to 2.3 for different systems.

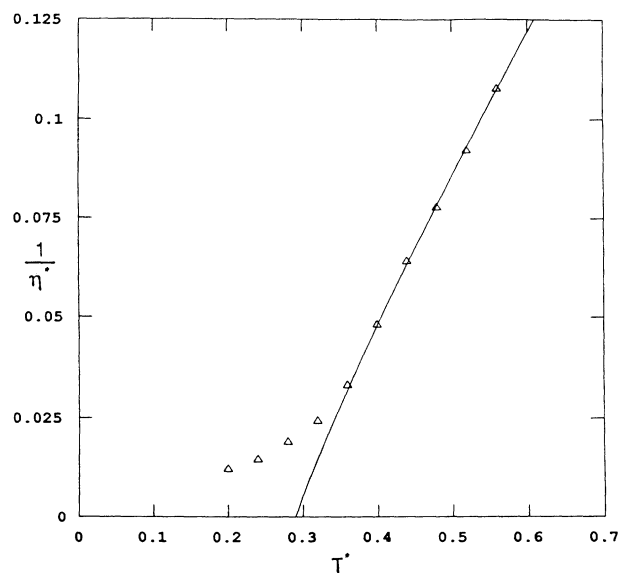


FIG. 6. Inverse of the shear viscosity  $\eta^*$ . The solid line corresponds to a power-law fit  $(T^* - T_g^*)^\alpha$  with  $T_g^* = 0.29$  and  $\alpha = 0.9$ , for  $T^* > 0.35$ .

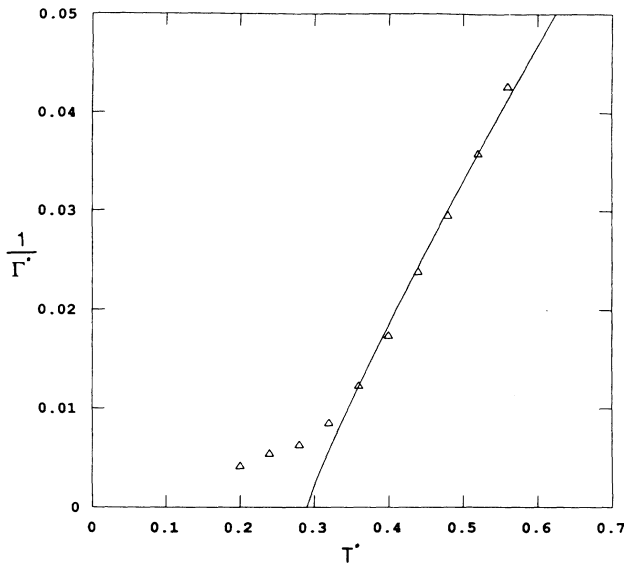


FIG. 7. Inverse of the longitudinal viscosity  $\eta^*$ . The solid line corresponds to a power-law fit  $(T^* - T_g^*)^\alpha$  with  $T_g^* = 0.29$  and  $\alpha = 0.9$ , for  $T^* > 0.35$ .

We can make a better comparison of our results with data from computer experiments done on LJ systems. In Ref. 13 a LJ fluid was cooled along the zero-pressure isobar and their calculated diffusion coefficient fits a power-law form  $(T^* - 0.29)^\alpha$  with  $\alpha = 2$ . The vanishing of the extrapolated diffusion coefficient at  $T^* = 0.29$  reflects the transition to a glassy phase. The power-law fit of our data in Figs. 6 and 7 (shown by solid lines) demonstrates similar behavior for high temperatures until the sharp transition is cut off in the low-temperature regime. Thus, apart from the poor matching between the exponents, our findings can be regarded as being in good agreement with results obtained from studies on computer liquids as well as having qualitative agreement with results for real liquids.

## VI. CONCLUSION

We have considered here a simple model for an isotropic compressible liquid and computed the contributions to the transport coefficients due to coupling of the density-fluctuation modes. In Ref. 5 a similar analysis was carried out in a much simpler but unphysical situation where the structure factor for the liquid had no wave-number dependence. In this work the wave-number dependence of the structure factor for the liquid is similar to that observed in real systems. As a direct consequence of this we were able to make contact between our results and those obtained from other studies on similar systems. In the flat-spectrum case there was no coupling between the shear viscosity and the density fluctuations, since such a coupling is generated by gradients of the density in the effective Hamiltonian  $F_u[\rho]$ . So in the present case we also obtain the mode-coupling contribution to the shear viscosity.

Recent work<sup>15</sup> by Bengtzelius treats the wave-vector dependence in the mode-coupling theory of the glass transition. This model was deduced from the kinetic theory of dense fluids. At high density it shows a sharp transition from an ergodic phase to a nonergodic phase. In this nonergodic phase the Laplace transform of the density correlation function has a  $1/w$  pole, which means that it decays to a nonzero value in the long-time limit. This is classified as an ideal glass. On the other hand, the model<sup>5</sup> we have discussed here was obtained from the equations of the nonlinear fluctuating hydrodynamics and is more general than any microscopic approach. In both the models the dominant mode-coupling contributions to the transport coefficients come from the density-fluctuation modes. However, in the later theory there is a mechanism that cuts off the sharp transition. At first the density fluctuations tend to drive the viscosity to large value. But for large viscosities the correlation function is proportional to  $1/(w + i\gamma q^2)$ , instead of  $1/w$ . Thus one obtains a diffusive mode, and there is no transition to an ideal glassy phase. The correlation function decays to zero with a lifetime inversely proportional to  $\gamma q^2$ . This diffusive mode comes from a careful analysis of the equations of NFH with the nonlinear constraint (2.1). This approach not only takes into account the coupling of the density-fluctuation modes but also incorporates the coupling between the currents and the density fluctuations in a compressible fluid. This can be seen more clearly from the expression (3.28), which involves both the current correlation function and the density correlation function. In the present work this model is extended to finite values of the wave vector in order to investigate the effect of the structure of the liquid on its dynamical behavior. We have considered here a simple LJ system and calculated how much its transport coefficients are enhanced due to the mode-coupling contributions. It should be pointed out here that we have extended the equations of the NFH to finite values of the wave vector in a simple way by choosing the form (2.10) for the free-energy functional; while this is a reasonable first step to take it is by no means a unique choice.

In Ref. 15 it is stated that when a simple LJ system is cooled along the zero-pressure isobar, it undergoes a glass transition at  $T = 0.477$ . Computer simulations on the same system along the  $P^* = 0$  isobar predict that a glass transition should occur at  $T_g^* = 0.29$ . The extrapolated self-diffusion coefficient goes to zero at this temperature. The data for the diffusion coefficient is found to agree quite well with a power-law fit  $(T^* - 0.29)^\alpha$  with  $\alpha = 2$ . In comparison with this, for  $T^* > 0.35$  our data for both the shear and the longitudinal viscosities also fit a power-law form very well around the "transition point"  $T_g^* = 0.29$  with an exponent  $\alpha = 0.9$ . As the temperature is further lowered, the sharp nature of the transition is cut off and the viscosity continues to increase at a slower rate. Thus, our results show a good agreement with the molecular-dynamics simulations.

The behavior described above is also qualitatively similar to that observed by Taborek, Kleiman, and Bishop<sup>3</sup> in a number of different laboratory systems which were referred to as fragile glasses in Ref. 1. However, in real

liquids one observes a much sharper enhancement of the viscosity over the same temperature region than we have seen here.

As a next step, it will be interesting to investigate how much the viscosity gets enhanced with the fall of temperature when other types of interaction potentials are considered. One can also compute the frequency-dependent transport coefficients to make comparisons with experiments<sup>31</sup> done by Nagel and coworkers.

We conclude this section with the following two points.

(i) In our work, the coupling constants in the mode-coupling terms given by Eqs. (3.25) and (3.26) are obtained from the equations of the nonlinear fluctuating hydrodynamics. These are quite different from the one given by Eq. (2.4) of Ref. 15. The latter was obtained by making approximations<sup>32</sup> in the kinetic theory of dense fluids.

(ii) We have calculated the structure factor for the liquid in the supercooled region with methods that are usually used for much higher temperatures. Whether this gives an accurate enough description of the structure of the supercooled liquid is an open question. A more care-

ful investigation of this point might provide further insight into the problem.

#### ACKNOWLEDGMENTS

I gratefully acknowledge Professor Gene F. Mazenko for his guidance, encouragement, and forbearance, and for his suggestion that I work on this problem. I would also like to thank Professor J. Douglas and Professor D. Oxtoby for valuable discussions. Thanks are due to Lee Brekke for his constant enthusiasm and useful conversations; to Joanne Cohn and William Sawyer for reading the manuscript; to Scott Anderson for helping with computers; and to all my friends and colleagues for their constant encouragement. This work was supported by the National Science Foundation under Grant No. DMR-84-12901 and by the National Science Foundation Materials Research Laboratory at The University of Chicago (Chicago, IL). This work was presented as a thesis to the Department of Physics, The University of Chicago, in partial fulfillment of the requirements for the Ph.D. degree.

\*Present address: Department of Physics, University of Florida, Gainesville, FL 32611.

<sup>1</sup>C. A. Angell, Proceedings of the Workshop on Relaxation Processes, Blacksburg, Va., July, 1983 (unpublished).

<sup>2</sup>C. A. Angell, J. H. R. Clarke, and L. V. Woodcock, *Adv. Chem. Phys.* **48**, 397 (1981); C. A. Angell, *Ann. N. Y. Acad. Sci.* **371**, 136 (1981); J. R. Fox and H. C. Anderson, *J. Phys. Chem.* **88**, 4019 (1984); J. J. Ullo and S. Yip, *Phys. Rev. Lett.* **54**, 1509 (1985).

<sup>3</sup>P. Taborek, R. N. Kleiman, and D. J. Bishop, *Phys. Rev. B* **34**, 1835 (1986).

<sup>4</sup>S. P. Das, G. F. Mazenko, S. Ramaswamy, and J. Toner, *Phys. Rev. Lett.* **54**, 118 (1985).

<sup>5</sup>S. P. Das and G. F. Mazenko, *Phys. Rev. A* **34**, 2265 (1986).

<sup>6</sup>L. Verlet, *Phys. Rev.* **165**, 202 (1968).

<sup>7</sup>E. Leutheusser, *Phys. Rev. A* **29**, 2765 (1984).

<sup>8</sup>U. Bengtzelius, N. Götze, and A. Sjölander, *J. Phys. C* **17**, 5915 (1984).

<sup>9</sup>D. Oxtoby, *J. Chem. Phys.* **85**, 1549 (1986); S. Sachdev, *Phys. Rev. B* **33**, 6395 (1986).

<sup>10</sup>G. F. Mazenko, S. Ramaswamy, and J. Toner, *Phys. Rev. Lett.* **49**, 51 (1982); *Phys. Rev. A* **28**, 1618 (1983).

<sup>11</sup>T. R. Kirkpatrick, *Phys. Rev. A* **31**, 939 (1985).

<sup>12</sup>J. P. J. Michels and N. J. Trappeniers, *Chem. Phys. Lett.* **66**, 20 (1979).

<sup>13</sup>J. H. R. Clarke, *J. Chem. Soc. Faraday Trans. 2.* **75**, 1371 (1979).

<sup>14</sup>C. Marchetti, *Phys. Rev. A* **33**, 3363 (1986).

<sup>15</sup>U. Bengtzelius, *Phys. Rev. A* **33**, 3433 (1986).

<sup>16</sup>R. Zwanzig and M. Bixon, *Phys. Rev. A* **2**, 2005 (1970).

<sup>17</sup>H. Mori, *Prog. Theor. Phys.* **49**, 1516 (1973).

<sup>18</sup>S.-k. Ma and G. F. Mazenko, *Phys. Rev. B* **11**, 4077 (1975).

<sup>19</sup>L. D. Landau and I. M. Lifshitz, *Course of Theoretical Physics* (Pergamon, New York, 1959), Vol. 6.

<sup>20</sup>J. Langer and L. Turski, *Phys. Rev. A* **8**, 3230 (1973).

<sup>21</sup>P. C. Martin, E. D. Siggia, and H. A. Rose, *Phys. Rev. A* **8**, 423 (1973).

<sup>22</sup>D. Forster, D. Nelson, and M. Stephen, *Phys. Rev. A* **16**, 732 (1977).

<sup>23</sup>J. D. Weeks, D. Chandler, and H. C. Anderson, *J. Chem. Phys.* **54**, 5237 (1971); H. C. Anderson, D. Chandler, and J. D. Weeks, *ibid.* **56**, 3812 (1972).

<sup>24</sup>J. P. Hansen and J. R. McDonald, *Theory of Simple Liquids* (Academic, London, 1976).

<sup>25</sup>M. S. Wertheim, *Phys. Rev. Lett.* **10**, 321 (1963); E. Thiele, *J. Chem. Phys.* **39**, 474 (1963); M. S. Wertheim, *J. Math. Phys.* **5**, 643 (1964).

<sup>26</sup>L. Verlet and J.-J. Weiss, *Phys. Rev. A* **5**, 939 (1972).

<sup>27</sup>N. W. Ashcroft and J. Lekner, *Phys. Rev.* **145**, 83 (1966).

<sup>28</sup>N. F. Carnahan and K. E. Starling, *J. Chem. Phys.* **51**, 635 (1969).

<sup>29</sup>P. Boon and S. Yip, *Molecular Hydrodynamics* (McGraw-Hill, New York, 1980).

<sup>30</sup>P. G. de Gennes, *Physica* **25**, 825 (1959).

<sup>31</sup>Y. H. Jeong, S. R. Nagel, and S. Bhattacharya, *Phys. Rev. A* **34**, 602 (1986); N. Birge and S. Nagel, *Phys. Rev. Lett.* **54**, 2674 (1985).

<sup>32</sup>G. F. Mazenko, *Phys. Rev. A* **9**, 360 (1974).